HHS Public Access

Author manuscript

Acc Chem Res. Author manuscript; available in PMC 2015 November 17.

Published in final edited form as:

Acc Chem Res. 2012 November 20; 45(11): 1927–1935. doi:10.1021/ar3001537.

Transport in supported polyelectrolyte brushes

Carmen Reznik[†] and **Christy F. Landes**[*]

Department of Chemistry, Rice University, Houston TX 77005

Conspectus

Functional polymers have a wide variety of applications ranging from energy storage to drug delivery. For energy storage applications, desirable material properties include low cost, high charge storage and/or mobility, and low rates of degradation. Isotropic thin films have been used for many of these types of applications, but research suggests that different structures such as polymer brushes can improve charge transport by an order of magnitude. Supported polymer brush structures produced by 'grafting-from' polymerization methods offer a framework for a controlled study of these materials on the molecular-scale. Using these materials, researchers can study the basis of hindered diffusion because they contain a relatively homogeneous polyelectrolyte membrane. In addition, researchers can use fluorescent molecular probes with different charges to examine steric and Coulombic contributions to transport near and within polymer brushes.

In this Account, we discuss recent progress in using fluorescence correlation spectroscopy, single-molecule polarization-resolved spectroscopy, and a novel 3-dimensional orientational technique to understand the transport of charged dye probes interacting with the strong polyanionic brush, poly(styrene sulfonate). Our preliminary experiments demonstrate that a cationic dye, Rhodamine 6G, probes the brush as a counterion, and diffusion is therefore dominated by Coulombic forces, which results in a ten-thousand-fold decrease in the diffusion coefficient in comparison with free diffusion. We also support our experimental results with molecular dynamics simulations. Further experiments show that up to 50 percent of the time, Rhodamine 6G translates within the brush without significant rotational diffusion, which indicates a strong deviation from Fickian transport mechanisms (In which translational and rotational diffusion are related directly through parameters such as chemical potential, size, solution viscosity, and thermal properties). To understand this oriented transport, we discuss the development of an experimental technique that allows us to quantify the 3-dimensional orientation on the time scale of intra-brush transport. This method allowed us to identify a unique orientational transport direction for Rhodamine 6G within the poly(styrene sulfonate) brush and to report preliminary evidence for orientational dye 'hopping.'

Graphical abstract

[*]To whom correspondence should be addressed. cflandes@rice.edu, (telephone)713-348-4232 (fax) 713-348-5155.
[†]current address: Shell Global Solutions, 3333 Highway 6 South, Houston, TX 77082-3101

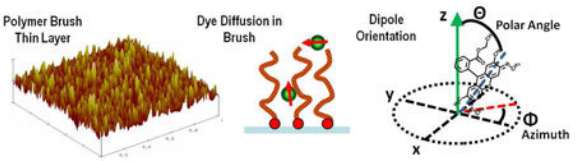

Introduction

Functional polymer films[1-5] are used in a wide variety of applications. One example is Nafion® (Dupont), a sulfonated polytetrafluoroethylene, as a proton exchange medium in polyelectrolyte membrane fuel cells[6]. An advantage of polymeric materials is that their composition can be engineered to exhibit dynamic or switchable physical, chemical, or electrical properties, particularly in the case of supported polymer brushes. It is therefore valuable to understand how chemical properties such as grafting density, polymer length, phase segregation, and polyelectrolyte strength relate to mass and ion transport within polymer brushes.

Desirable properties for energy storage applications include low cost, high charge storage and/or mobility, and low rates of degradation. Nafion® (Dupont) exhibits high charge mobility and low tendency to degrade. Unfortunately, it is also expensive and not environmentally friendly. There are a variety of possible polyelectrolyte alternatives[7-10], including poly(styrene sulfonate) (PSS)[11-14]. It has been shown that both polyelectrolyte nanostructure and local solvation dynamics affect ion transport efficiencies[15], and these properties are targets for potential fuel cell membrane design improvements[16,17]. Potential problems include loss of conductivity due to excessive swelling or higher order charge interactions[11,18,19]. Various synthetic strategies have been employed to overcome these problems and optimize properties, including polymer crosslinking[11,20], functionalization[21], and advanced grafting techniques[22-24].

Our practical knowledge of how to prepare polymeric materials vastly exceeds our understanding of the molecular-scale processes that govern transport in charged and crowded media. For example, it has been shown that by switching from isotropic thin films (Figure 1A) to supported polymer brushes (Figure 1B) it is possible to improve transport efficiencies by over an order of magnitude. This effect is thought to be due to the increase in molecular ordering[25] achieved in a polymer brush by end-grafting polymer chains to a surface.

The highly disparate experimental and theoretical studies of complex fluid networks in general and polyelectrolyte films in particular share a general overall conclusion: their chemical properties depend strongly on the local polymer structure and degree of water solvation[12,18,26-43]. One suggested Nafion film morphology, a lamellar structure[26], is depicted in Figure 1C, in which the hydrophilic water-solvated sulfonate regions phase-separate from the hydrophobic fluorinated polymer backbone. Also, the mechanism of solute hopping[36] within and between hydrophilic networks has been theoretically suggested as a viable transport mechanism within polyelectrolyte films. Despite advances in both the measurement of ion/polymer brush interactions[18,19], and the modeling of complex

fluids[44-47], there remains a lack of mechanistic detail about the interplay of local solvation dynamics, cooperativity, pore size, and transport efficiency.

Mechanistic details can be acquired by studying transport in polyelectrolyte brushes at the single molecule level. In this account, we discuss our recent findings regarding transport in charged and crowded PSS brushes, and the development of analytical techniques required for these experiments. First, the basic sample and experimental system are described. Next, we discuss our initial finding that transport of counterion probes in the presence of the PSS brush is slowed by orders of magnitude, and that this is primarily due to electrostatic interactions. Further, single molecule polarization anisotropy analysis reveals heterogeneous transport mechanisms, and suggests that oriented transport occurs in the brushes. This finding necessitates the development of a novel technique that allows three-dimensional orientational dynamics to be extracted, and we detail the progress towards this goal. Finally, we offer some insights on the outstanding questions that must be addressed in order to engineer molecular ion transport in these systems.

Description of Samples and Basic Experimental Setup

We conducted some of the first work using FCS to evaluate diffusion near and in ordered polymer brush thin films, reporting on diffusion characteristics of charged molecular ions interacting with PSS polymer brushes. A schematic of the epiflourescence microscope is shown in Figure 2.a, and details of the method are provided in the literature[39,48,49]. The polymer brushes are supported on a glass surface, and grown via an asymmetric surface-grafted initiator into thin films that are densely packed and more homogeneous in length and density than can be accomplished with alternate thin-film preparation methods. The surface-initiated polymerization of PSS used in these studies yields grafting densities of approximately 0.05 nm[2,37,50,51]. As can be seen in the cartoon in Figure 2b, for densely grafted polymer strands, the distance between grafting spots is smaller than the radius of gyration of the polymer strand, and therefore inter-strand repulsion causes the polymer chains to extend and adopt a general orientation vector that is normal to the surface. PSS, a strong polyelectrolyte, is deprotonated at all pHs reported in this work (pH > 1), and Coulombic repulsion contributes to extension and ordering of the polymer strands. Figures 2.d and 2.e show representative surfaces as evaluated by AFM for a clean coverslip (2.c) and a surface modified with polymer brush (2.d).

For FCS measurements on thin films, it is important to address the heterogeneous environment that exists in the laser focal volume. Figure 2.b depicts the intersection of a laser focal volume with the polymer brush thin film. What is evident from the cartoon is that the laser focal volume encompasses: 1) the polymer brush, 2) an interfacial region, and 3) bulk solvent. Note that in this image, the dimension of the thin film normal to the surface (along the z axis) is exaggerated; the thin films we study have dry thicknesses from 10 to 50 nm, while the focal volume dimension along the z axis is ~ 2 μm. For details as to data acquisition and analysis, the reader is directed towards the published original work and associated Supplementary Information[39]. The overall results are described briefly below.

Transport of Fluorescent Probes in Pss Brush

The most significant initial result is that diffusion of a counterion probe is slowed by orders of magnitude in the presence of the PSS brush. Three fluorescent dyes, cationic Rhodamine 6G, neutral Bodipy-R6G, and anionic Alexa 555, differ in their extent and intensity of interaction with the polyanionic PSS polymer brush, as indicated by extracted diffusion times. The fitted autocorrelation expression is used to extract the characteristic diffusion time for each analyte[48,52]. Average diffusion times for the dyes through the FCS confocal laser volume in bulk solution are in the 20 to 30 μs time scale (R6G 25 μs, Bodipy 22 μs, Alexa 32 μs). When the dyes diffuse in the presence of polymer brush, multiple diffusion times are observed, as reported in Table 1. From the table, we see that only anionic Alexa 555 exhibits a detectable level of bulk-like diffusion, in contrast to R6G and Bodipy, which show a negligible level of bulk-like diffusion when the brush is present. The strong interaction between positively charged R6G and the negatively charged polymer brush causes R6G to interact almost exclusively with the brush. Assuming equivalent brightness for all R6G molecules regardless of diffusion time, an evaluation of the autocorrelation amplitudes of the diffusion components suggests that 92% of the diffusion occurs at timescales that are four orders of magnitude slower than bulk diffusion.

Although Alexa is anionic, it does exhibit interaction with the polymer brush, as indicated by the presence of a diffusion component ~ 75 times slower than bulk diffusion. Again, assuming equivalent brightness for the molecules, Alexa 555 interaction with the brush constitutes about 45% contribution to diffusion. The neutral Bodipy's interaction with the polymer brush is strong enough to render bulk-like diffusion undetectable. Relative amplitudes for slow and intermediate diffusion are 58% and 42%, consistent with a weaker interaction with the brush than observed for R6G.

The data suggests that with the three dyes, we measure diffusion occurring across three distinct environments that exist in this system: diffusion within the body of the brush, at the interface, and in bulk solution. Bulk solvent diffusion can be assumed for the μs time scale component, due to consistency with measurements made in the absence of polymer brush. We assign the slowest transport for both R6G and Bodipy to diffusion of the dyes within the brush membrane[39], whereas the small contribution of intermediate diffusion on the millisecond time scale could be due to surface interactions. Single molecule intensity fluctuations and rotational anisotropy data, discussed later, support these assignments[53]. In the case of Alexa diffusion, the slow diffusion component may be attributed to an interaction of the negatively charged dye with an electrical double layer formed at the surface of the negatively charged polymer brush thin film[54-56]. Other diffusion studies, performed on a variety of polymer brushes prepared by different techniques, find that slow counterion probe diffusion may primarily be due to interactions with the outermost portions of the polymer brush[41]. Overall, the investigation of diffusion of counterion probes interacting with PSS brushes might provide needed insight on ion storage/release.

Additionally, that the slowest diffusion component of R6G is four times slower than that of BODIPY, is an indication that in addition to steric factors, electrostatic forces are involved

in the diffusion of the cationic R6G in the PSS brush. pH-dependent experimental analysis and simulations support a role for electrostatic-mediated transport[39].

Decoupling of Translational and Rotational Diffusion in Pss Brush

Polarization resolved spectroscopy of single molecules provides a means to evaluate molecular orientation, and thus provides an added tool for evaluating molecular interactions within the polymer brush system. Previously, this tool has been used extensively to evaluate rotational behavior of molecules embedded in materials where molecules are translationally stationary and where rotational diffusion is on the order of hundreds of milliseconds to tens of seconds. By employing two detectors and a polarization beam splitting cube in the FCS detection path (Figure 1.a), we evaluated the orientation adopted by *translationally diffusing* single molecules in solvated PSS polymer brushes. A quantity known as the linear dichroism, given in equation (1), can be calculated from orthogonal fluorescence intensity traces, I_p and I_s, collected for diffusing molecules as a function of time:

$$A(t)=\frac{I_p(t)-I_s(t)}{I_p(t)+I_s(t)}. \quad (1)$$

Figure 3.a shows specific details of the detection scheme employed. The probability that a photon with a certain orientation will pass through the polarization beam splitting cube and proceed either to the s or p detector is dependent on its orientation with respect to the x-y plane, as $cos^2\Phi$.

Time dependent intensity traces of the orthogonal polarization data are shown in Figures 3.b-d, and the data is used to calculated *A(t)*. *A(t) c*an be used as a metric to follow the change in time of single molecule orientation.

Diffusion of R6G in the polymer brush provides an opportunity for evaluation of the rotational motion of translating single molecules in the brush medium, because of the strong interaction between R6G and PSS. The time scale for translational diffusion when R6G is associated with the brush is slow enough to allow collection of adequate signal for evaluation of the linear dichroism, and as our data shows, the rotational diffusion time scale is often also slow enough as well, to be resolved with the detection system employed. It should be noted that a typical rotational time scale for a molecule interacting with a medium possessing viscosity as calculated for the polymer brush, is fast enough to be well beyond the time scale of our data binning; (rotational time scales can be estimated to be at maximum on the order of 100 us, with data binning at 1 ms[53].

The single R6G diffusion trajectories in PSS reveal the existence of multiple distinct modes of motion. It should be noted that of the trajectories shown in Figure 3 are representative of many thousands of diffusion events observed in data collected over more than 30 minutes, and evaluated via automated algorithms[53]. In the trajectories shown in Figure 3, individual detector traces are shown in the bottom panel and the total intensity traces are plotted in the top panel. For molecules rotating faster than the data collection time scale, signal counts on all channels will be approximately equal, and the mean values of *A(t)* will approach 0. This

is the case for the region numbered 2 in Figure 3.c., indicating fast rotation of the molecule, while diffusion in the focal volume over this region is indicated by the changing intensity profile. In the regions numbered 1 and 3 in Figures 3.c and d, the value of *A(t)* is 0.4663 and 0.4508, indicating orientation is maintained over long time periods. At region 1, we observe an example of a trajectory for which the total intensity profile is changing while significant orientation is maintained. There are multiple causes for changing total intensity with maintained orientation, namely a molecule that is translationally stationary but rotating slowly with respect to the z axis (see the coordinate system defined in Figure 3.a), or a translationally diffusing molecule that maintains a significant degree of orientation, as may occur via interaction of R6G with polymer strands that exhibit an average orientation vector. In Figures 3.b, and d, the total intensity profile remains stable for many tens of milliseconds, indicating adsorption of the dye molecules on the polymer brush. In Figure 3.b, rapid switching between polarization states for the molecule is observed during the adsorption event. In this figure, the linear dichroism is plotted in the center panel, and it can be seen that the linear dichroism shows long periods with an essentially stationary value consistent with adsorption. However, the linear dichroism also shows rapid switching of values that occurs in discrete steps. Such switching suggests that in between adsorbed states, there are brief moments when the molecule is released to rotate on a time scale that is more rapid that the 1 ms time resolution of the detection system, after which it readsorbs.

The single molecule studies evaluating orthogonal polarization of emitted light reveal heterogeneous modes of transport within the PSS brush system, and also demonstrate a dynamic association between the dye and the PSS brush. That we observe oriented transport initiates the question: in which direction does oriented transport occur? In order to answer this question, it is necessary to develop a method to monitor transport in three dimensions, with micro to millisecond time resolution, a time scale inaccessible by established wide-field methods for monitoring such motion.

3D Orientational Dynamics of Probes in Pss Brush

By observing diffusion of R6G using 3-angle polarization resolved detection[57], we are able to uncover further details of the transport mechanisms because this technique provides information about molecular orientation with respect to the z axis in addition to orientation with respect to the x-y plane. Figure 4.a shows the spherical coordinate scheme used. The use of high numerical aperture optics along with three detectors equipped with polarization filters so as to detect emission light at three different polarization angles allows discernment of the spherical coordinates[58,59]. Details of the equations used to determine these coordinates as a function if intensity measured at the three detectors are outlined in our 2011 publication on this work[57].

The method provides a significant advantage in evaluating transport in structurally ordered systems in which orientation vectors lay along the z axis. In addition to resolving the full orientational details for individual molecules, another advantage of this technique is that the time resolution is determined by photon collection hardware and is thus greatly increased over the time resolution of imaging hardware that has been traditionally used for 3-D orientation mapping of translationally stationary single molecules.

The detection scheme is as shown in Figure 2.a, with the addition of a 50/50 beam splitter before the two detectors shown, splitting light to an additional detector with a polarization filter set to 45° (for full details, see Ref. #[57]). Representative data acquired from the 3-detectors for a single diffusion event with R6G diffusing in the polymer brush are shown in Figure 4.b. For the purpose of analysis, rapid rotation/reorientation, which is evident in regions for which there is equal signal on all three channels, is termed 'Type 1' reorientation. Oriented periods marked by significant inequality among the three channels indicating restricted rotation, is termed 'Type 2' reorientation. Note that Type 1 traces can arise from freely rotating molecules and also from molecules that are oriented with polar angle Θ close to 0, with $\Theta = 0$ assigned as the excitation and observation axis of the microscope.

Based on the characteristics of the intensity traces, it is possible to build trajectory analysis algorithms using the equations outlined in our previous work in order to automate evaluation of full trajectories lasting many minutes and which are composed of thousands of diffusion events. The algorithms find, identify and isolate Types 1 (rapid rotational diffusion) and Type 2 (restricted rotational diffusion) motions. By using these algorithms, we were able to collect data on the distribution of angles experienced by single molecules during the two distinctive Type 1 and Type 2 reorientation regimes. These data are shown in Figure 4.c, where histograms of the spherical coordinates for Type 1 (in purple) and Type 2 (in red) are plotted for a five minute diffusion trace. The calculated azimuthal angles (left) and polar angles (right) are shown.

The azimuthal angle distribution for Type 1 diffusion is relatively smooth, with peaks at ±45°, as expected for a freely rotating dipole. The polar angle distribution is centered at values around ∼23°, also typical for free rotation. The polar angle distribution center occurs due to a combination of fast rotation, averaged over all angles, and contributions from molecular orientations near $\Theta = 0°$. The azimuthal angle distribution arises from some instances of molecular orientations near $\Phi = 45°$, and predominantly from fast rotation which, again, presents the same intensity profile.

Distributions for oriented, Type 2 diffusion, on the other hand, are non-uniform, with the azimuthal distribution centered at 12° for one brush sample, and shifted polar angle distribution centered at 39°. Over all, the clustering of angle values for Type 2, oriented, diffusion events, suggests a strong preferential orientation for R6G dye molecules that are interacting strongly with the PSS brush. Such preferential orientation is not observed for R6G imbedded in an isotropic PMMA polymer film[57]; and thus the observed orientational preference in the PSS film can be ascribed to an orienting director of the polymer brush. Both steric and Coulomb interactions between the dye and brush potentially contribute to an average alignment of R6G with the brush orientation vector. Support for this conclusion is provided by simulations, as discussed below.

As depicted in Figure 5, orientational switching, outside of the changes that would be expected for instrumental noise, can be observed for R6G in PSS. Observed reorientation of translationally stationary R6G molecules embedded in a spun-cast, isotropic PMMA thin film serves as a control. In Figure 5, three kinds of data are plotted: 1) intensity as a function

of time (parts a and d), 2) angle distributions over the events shown in a and d (parts b and e), and 3) a time progression of orientation (parts c and f). On the left, the data is collected over several translationally stationary single molecules embedded in PMMA (parts a-c), and on the right, the data shown is for several single molecule diffusion events in PSS brush (parts d-f).

It is known that molecules embedded in PMMA thin films exhibit very slow rotation[60], and our data confirm that we can detect such behavior. The angle distributions shown for the rotationally restricted molecules in PMMA in 5.b are narrower than those for diffusing molecules in the PSS brush, plotted in 5.e. In Figures 5.c and f, the time progressions of molecular orientation for the traces in the top panels of 3.a and c are plotted. For PMMA, (5.c) we observe a 56 ms span in which the probe is stationary (highlighted). Over this period of time, θ and ϕ fluctuate by ~5% with mean values of $<\theta> = 6.2°$ and $<\phi> = 56.9°$. By evaluating rotationally stationary regions identified across several events, an estimation of experimental noise limits for angle resolution can be made and is ±5° for angles from $-45° < \phi < 45°$ and $23° < \theta < 75°$.

Dipole reorientation can be identified for angle movements that extend beyond noise-limited fluctuations. Switching of dipole orientation is observed in a class of single molecule events observed in the PSS system. The transient oscillations of dipole orientation in the θ/ϕ space are seen to occur during strong interactions where rotation is restricted, which is highlighted in 5.f, over a span of 56 ms in which oscillations occur with an approximate period of 9 ms. Transient occupation of local energy ‘metabasins’ in the PSS thin film structure may contribute to oscillatory behavior.[61,62]

Summary and Outlook

The most important general conclusion of this work is that, although fluorescent probes are large compared with protons shuttled in fuel cell applications, the study of inter-brush solvation of single counterion probes provides a method by which to test the disparate hypotheses about transport inside polymer films. Transport of counterion probes within an ordered strong polyelectrolyte film is strongly influenced by both electrostatics and sterics. Oriented translation and orientational hopping have been experimentally identified. Such heterogeneous transport behavior raises the question as to whether such oriented motion occurs between polymer chains, in lateral solute hopping, or along chains, in axial hopping. In order to answer this question, a 3-D polarization resolved single molecule apparatus is constructed. The preliminary results from this experiment demonstrate the utility of the method for acquiring 3D orientational dynamics and identifying a unique orientational direction for each PSS brush. Other important results are provided by detailed simulations, which make possible the identification, quantification, and classification of oriented translational diffusion mechanisms.

Now that we have identified oriented transport dynamics and established methods to quantify this property in supported polyelectrolyte films, two open questions must be addressed. First, it is important to experimentally determine the relative contribution of axial vs. lateral transport as a function of brush density, hydration, and length, and to establish if

oriented transport can be optimized for charge storage/release properties. Also, detailed molecular dynamics simulations that address the multiscalar relationships between solute mobility and higher order polymer motions are necessary. Current efforts are underway to address these questions.

Acknowledgments

C. Landes thanks the Norman Hackerman Welch Young Investigator Program at Rice University, the National Science Foundation [Grants CBET-1133965 and CHE-1151647], and the National Institutes of Health [Grant GM94246-01A1], as well as the Donors of the American Chemical Society Petroleum Research Fund for partial support of this research. C. Reznik thanks the Houston Area Molecular Biophysics program for partial support of this work. We also thank Prof. Rigoberto Advincula and his research group for the polymer brush initiator synthesis and characterization, and Prof. Stephan Link and his research group for helpful discussions and suggestions.

References

1. Padeste C, Farquet P, Potzner C, Solak HH. Nanostructured bio-functional polymer brushes. J Biomat Sci, Poly Ed. 2006; 17:1285–1300.
2. Tu H, Hong L, Anthony SM, Braun PV, Granick S. Brush-sheathed particles diffusing at brush-coated surfaces in the thermally responsive PNIPAAm system. Langmuir. 2007; 23:2322–2325. [PubMed: 17261038]
3. Spruijt E, Choi EY, Huck WTS. Reversible Electrochemical Switching of Polyelectrolyte Brush Surface Energy Using Electroactive Counterions. Langmuir. 2008; 24
4. Wang M, Zoi S, Guerin G, Shen L, Deng K, Jones M, Walker GC, Scholes GD, Winnik MA. A Water-Soluble pH-Responsive Molecular Brush of Poly(N,N-dimethylaminoethyl methacrylate) Grafted Polythiophene. Macromolecules. 2008; 41:6993–7002.
5. Advincula, R.; Ruehe, J.; Brittain, W.; Caster, K. Polymer Brushes. VCH-Wiley; Weinheim: 2004.
6. Banerjee S, Curtin DE. Nafion perfluorinated membranes in fuel cells. J Fluorine Chem. 2004; 125:1211–1216.
7. Mermut O, Barrett CJ. Effects of charge density and counterions on the assemby of polyelectrolyte multilayers. J Phys Chem B. 2003; 107:2525–2530.
8. Mendelsohn JD, Barrett CJ, Chan VV, Pal AJ, Mayes AM, Rubner MF. Fabrication of microporous thin films from polyelectrolyte multilayers. Langmuir. 2000; 16:5017–5023.
9. Peng G, Genzer J, Szleifer I. Phase behaviour and charge regulation of weak polyelectrolyte grafted layers. Physical Review Letters. 2007; 98:018302. [PubMed: 17358511]
10. Lufrano F, Squadrito G, Patti A, Passalacqua E. Sulfonated polysulfone as promising membranes for polymer electrolyte fuel cells. J Appl Polym Sc. 2000; 77:1250–1257.
11. Chen S, Krishnan LSS, Benziger J, Bocarsly AB. Ion exchange resin/polystyrene sulfonate composite membranes for PEM fuel cells. J Membrane Sci. 2004; 243:327–333.
12. Gummel J, Cousin F, Boue F. Counterions release from electrostatic complexes of polyelectrolytes and proteins of opposite charge: A direct measurement. J Am Chem Soc. 2007; 129:5806–5807. [PubMed: 17439127]
13. Cayre OJ, Chang ST, Velev OD. Polyelectrolyte diode: nonlinear current response of a junction between aqueous ionic gels. J Am Chem Soc. 2007; 129:10801–10806. [PubMed: 17691778]
14. Bratko D, Kelbl A. Temperature dependence of the electrolytic conductivity of poly(styrenesulfonate) solutions. Macromolecules. 1986; 19:2083–2085.
15. Choi EY, Azzaroni O, Cheng N, Zhou F, Kelby T, Huck WTS. Electrochemical characteristics of polyelectrolyte brushes with electroactive counterions. Langmuir. 2007; 23:10389–10394. [PubMed: 17760471]
16. Norsten TB, Guiver MD, Murphy J, Astill T, Navessin T, Holdcroft S, Frankamp BL, Rotello VM, Ding J. Highly fluorinated comb-shaped copolymers as proton exchange membranes (PEMs): improving PEM properties through rational design. Adv Funct Mater. 2006; 16:1814–1822.

17. Pharoah JG, Karan K, Sun W. On effective transport coefficients in PEM fuel cell electrodes: anisotropy of the porous transport layers. J Power Sources. 2006; 161:214–224.
18. Bohme U, Scheler U. Hydrodynamic size and charge of polyelectrolyte complexes. J Phys Chem B. 2007; 111:8384–8350.
19. Pristinski D, Kozlovskaya V, Sukhishvili SA. Fluorescence correlation spectroscopy studies of diffusion of a weak polyelectrolyte in aqueous solutions. Journal of Chemical Physics. 2005; 122:014907/1–014907/9.
20. Chang DP, Dolbow JE, Zauscher S. Switchable friction of stimulus-responsive hydrogels. Langmuir. 2007; 23:250–257. [PubMed: 17190511]
21. Peng B, Johannsmann D, Ruhe J. Polymer brushes with liquid crystalline side chains. Macromolecules. 1999; 32:6759–6766.
22. Wu T, Gong P, Szleifer I, Vlcek P, Subr V, Genzer J. Behavior of surface-anchored poly(acrylic acid) brushes with grafting density gradients on solid substrates: 1. Experiment. Macromolecules. 2007; 40:8756–8764.
23. Ejaz M, Yamamoto S, Tsujii Y, Fukuda T. Fabrication of patterned high-density polymer graft surfaces. 1. Amplification of phase-separated morphology of organosilane blend monolayer by surface-initiated atom transfer radical polymerization. Macromolecules. 2002; 35:1412–1418.
24. Xu C, Wu T, Drain CM, Batteas JD, Fasolka MJ, Beers KL. Effect of block length on solvent response of block copolymer brushes: Combinatorial study with block copolymer brush gradients. Macromolecules. 2006; 39:3359–3364.
25. Whiting GL, Snaith HJ, Khodabakhsh S, Andreasen JW, Breiby DW, Nielsen MM, Greenham NC, Friend RH, Huck WTS. Enhancement of charge-transport characteristics in polymeric films using polymer brushes. Nano Lett. 2006; 6:573–578. [PubMed: 16522065]
26. Dura, JA.; Murthi, VS.; Hartman, M.; Satija, SK.; Majkrzak, CF. Macromolecules. Vol. 42. Washington, DC, United States: 2009. Multilamellar Interface Structures in Nafion; p. 4769-4774.
27. Bass, M.; Berman, A.; Singh, A.; Konovalov, O.; Freger, V. Macromolecules. Vol. 44. Washington, DC, United States: 2011. Surface-Induced Micelle Orientation in Nafion Films; p. 2893-2899.
28. Knox CK, Voth GA. Probing Selected Morphological Models of Hydrated Nafion Using Large-Scale Molecular Dynamics Simulations. J Phys Chem B. 2010; 114:3205–3218. [PubMed: 20158234]
29. Allahyarov E, Taylor PL. Simulation study of the equilibrium morphology in ionomers with different architectures. Journal of Polymer Science, Part B: Polymer Physics. 2011; 49:368–376.
30. Allahyarov E, Taylor PL, Lowen H. Simulation study of field-induced morphological changes in a proton-conducting ionomer. Physical Review E: Statistical, Nonlinear, and Soft Matter Physics. 2010; 81:031805/1–031805/11.
31. Gebel G. Structural evolution of water-swollen perfluorosulfonated ionomers from dry membrane to solution. Polymer. 2000; 41:5829–5838.
32. Hwang GS, Kaviany M, Gostick JT, Kientiz B, Weber AZ, Kim MH. Role of water states on water uptake and proton transport in Nafion using molecular simulations and bimodal network. Polymer. 2011; 52:2584–2593.
33. Schmidt-Rohr K, Chen Q. Parallel cylindrical water nanochannels in Nafion fuel-cell membranes. Nat Mater. 2008; 7:75–83. [PubMed: 18066069]
34. Kongkanand A. Interfacial water transport measurements in Nafion thin films using a quartz-crystal microbalance. Journal of Physical Chemistry C. 2011; 115:11318–11325.
35. Iyer ESS, Datta A. Importance of Electrostatic Interactions in The Mobility of Cations in Nafion. J Phys Chem B. 2011; 115:8707–8712. [PubMed: 21650467]
36. Devanathan R, Venkatnathan A, Rousseau R, Dupuis M, Frigato T, Gu W, Helms V. Atomistic Simulation of Water Percolation and Proton Hopping in Nafion Fuel Cell Membrane. J Phys Chem B. 2010; 114:13681–13690. [PubMed: 20860379]
37. Michailidou VN, Loppinet B, Prucker O, Ruehe J, Fytas G. Cooperative diffusion of end-grafted polymer brushes in good solvents. Macromolecules. 2005; 38:8960–8962.

38. Zhou F, Hu H, Yu B, Osborne VL, Huck WTS, Liu W. Probing the responsive behavior of polyelectrolyte brushes using electrochemical impedance spectroscopy. Anal Chem. 2007; 79:176–182. [PubMed: 17194136]
39. Reznik C, Darugar Q, Wheat A, Fulghum T, Advincula RC, Landes CF. Single ion diffusive transport within a poly(styrene sulfonate) polymer brush matrix probed by fluorescence correlation spectroscopy. J Phys Chem B. 2008; 112:10890–10897. [PubMed: 18630854]
40. Wang S, Zhu Y. Molecular diffusion on surface tethered polymer layers: coupling of molecular thermal fluctuation and polymer chain dynamics. Soft Matter. 2010; 6:4661–4665.
41. Zhang C, Chu X, Zheng Z, Jia P, Zhao J. Diffusion of Ionic Fluorescent Probes atop Polyelectrolyte Brushes. J Phys Chem B. 2011; 115:15167–15173. [PubMed: 22082148]
42. Dimitrov DI, Klushin LI, Milchev A, Binder K. Flow and transport in brush-coated capillaries: A molecular dynamics simulation. Physics of Fluids. 2008; 20
43. Egorov SA. Interactions between polymer brushes in solvents of variable quality: A density functional theory study. Journal of Chemical Physics. 2008; 129:064901/1–064901/8. [PubMed: 18715103]
44. Mason TG. Estimating the viscoelastic moduli of complex fluids using the generalized Stokes-Einstein equation. Rheol Acta. 2000; 39:371–378.
45. Liu Q, Kee DD. Modeling of diffusion through polymeric membranes. Rheol Acta. 2005; 44:287–294.
46. Wei CYJ, Kim YH, Darst RK, Rossky PJ, Vanden Bout DA. Origins of nonexponential decay in single molecule measurements of rotational dynamics. Physical Review Letters. 2005; 95:173001/1–173001/4. [PubMed: 16383825]
47. Wei CYJ, Lu CY, Kim Yeon H, Vanden Bout David A. Determining if a system is heterogeneous: The analysis of single molecule rotational correlation functions and their limitations. J Fluoresc. 2007; 17:797–804. [PubMed: 17703348]
48. Aragon S, Pecora R. Fluorescence correlation spectroscopy as a probe of molecular dynamics. Journal of Chemical Physics. 1976; 64:1791.
49. Eigen M, Rigler R. Sorting single molecules: application to diagnostics and evolutionary biotechnology. Proc Natl Acad Sci USA. 1994; 91:5740–7. [PubMed: 7517036]
50. Prucker O, Ruhe J. Polymer layers through self-assembled monolayers of initiators. Langmuir. 1998; 14:6839–6898.
51. Filippidi E, Michailidou V, Loppinet B, Ruehe J, Fytas G. Brownian diffusion close to a polymer brush. Langmuir. 2007; 23:5139–5142. [PubMed: 17367177]
52. Haustein E, Schwille P. Ultrasensitive investigations of biological systems by fluorescence correlation spectroscopy. Methods. 2003; 29:153–166. [PubMed: 12606221]
53. Reznik C, Estillore N, Advincula RC, Landes CF. Single Molecule Spectroscopy Reveals Heterogeneous Transport Mechanisms for Molecular Ions in a Polyelectrolyte Polymer Brush. J Phys Chem B. 2009; 113:14611–14618. [PubMed: 19813742]
54. Daniels CR, Reznik C, Landes CF. Dye Diffusion at Surfaces: Charge Matters. Langmuir. 2010; 26:4807–4812. [PubMed: 20163084]
55. Morel, F.; Hering, J. Principles and Applications of Aquatic Chemistry. John Wiley and Sons; New York: 1993.
56. Stumm, W.; Morgan, JJ. Aquatic Chemistry: Chemical Equilibria and Rates in Natural Waters. 3rd. John Wiley and Sons; New York: 1993.
57. Reznik C, Berg R, Foster E, Advincula R, Landes CF. Transient three-dimensional orientation of molecular ions in an ordered polyelectrolyte membrane. Journal of Physical Chemistry Letters. 2011; 2:592–598.
58. Fourkas JT. Rapid determination of the three-dimensional orientation of single molecules. Opt Lett. 2001; 26:211–213. [PubMed: 18033550]
59. Lu CY, Vanden Bout DA. Analysis of orientational dynamics of single fluorophore trajectories from three-angle polarization experiments. Journal of Chemical Physics. 2008; 128:244501/1–244501/10. [PubMed: 18601343]

60. Bartko AP, Xu K, Dickson RM. Three-dimensional single molecule rotational diffusion in glassy state polymer films. Physical Review Letters. 2002; 89:026101/1–026101/4. [PubMed: 12097008]

61. Adhikari AN, Capurso NA, Bingemann D. Heterogeneous dynamics and dynamic heterogeneities at the glass transition probed with single molecule spectroscopy. Journal of Chemical Physics. 2007; 127:114508/1–114508/9. [PubMed: 17887858]

62. Doliwa B, Heuer A. Hopping in a supercooled Lennard-Jones liquid: Metabasins, waiting time distribution, and diffusion. Physical Review E: Statistical, Nonlinear, and Soft Matter Physics. 2003; 67:030501/1–030501/4.

Biographies

Carmen Reznik graduated from Rice University with a Ph.D. in physical chemistry in 2011, and is currently working for Shell Global Solutions in Houston, Texas, in the field of Enhanced Oil Recovery. World energy needs remain a key interest, along with a few other things that include family, sailing and live music.

Christy F. Landes is an Assistant Professor in the Department of Chemistry at Rice University in Houston, TX. After graduating from George Mason University in 1998, she received a Ph.D. in Physical Chemistry from the Georgia Institute of Technology in 2003. She was a postdoctoral researcher at the University of Oregon and an NIH postdoctoral fellow at the University of Texas at Austin before joining the University of Houston as an assistant professor in 2006. She moved to her current position at Rice in 2009, earning an NSF CAREER award for her tenure-track work in 2011.

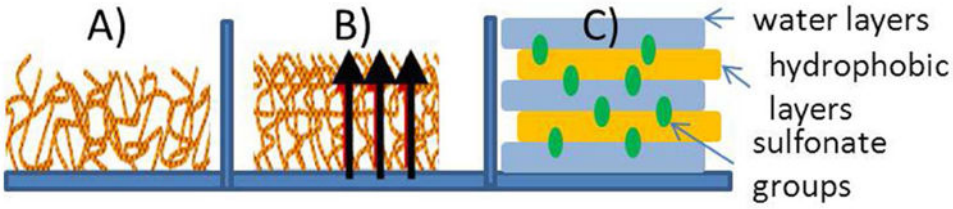

Figure 1. Polymer thin films

A) isotropic film, with varied internal structure; B) end-grafted polymer brush, with dense, ordered internal structure due to electrostatic repulsion; C) depiction of proposed phase-segregation and formation of lamellae in spin-cast Nafion (inspired by [26]).

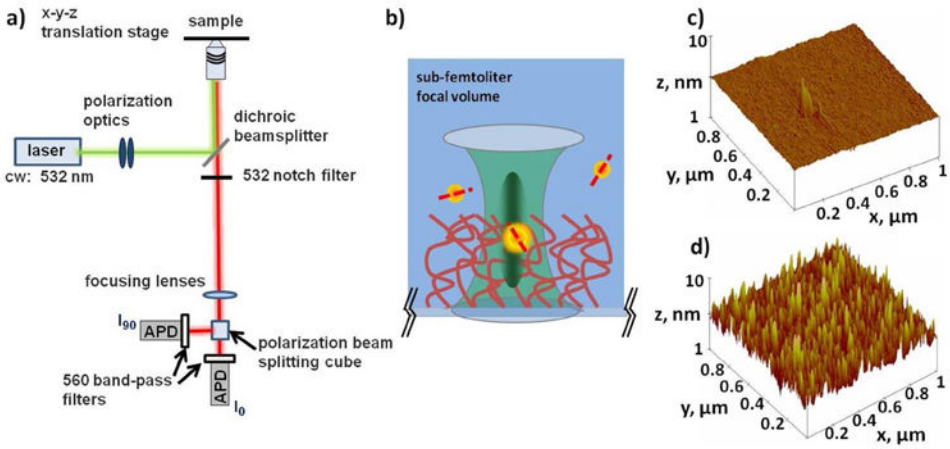

Figure 2.

a) Schematic of epiflourescence microscope. b) Cartoon showing the intersection of the laser focal volume with a polymer brush, and diffusing molecules with emission dipoles depicted (not to scale). c) AFM image of the surface of a clean coverslip. d) AFM image of a polymer brush modified coverslip.

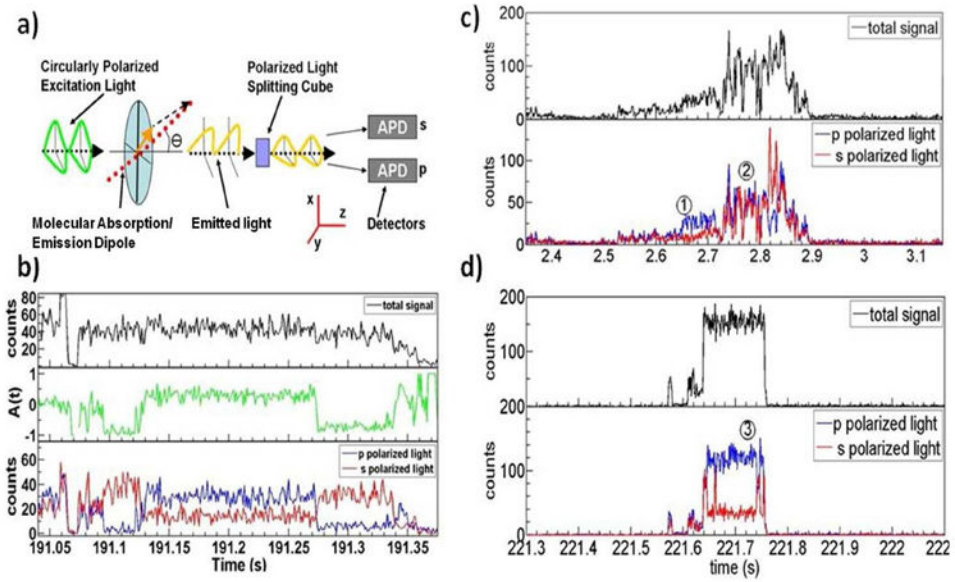

Figure 3.

a) Detection scheme for polarized light emitted from a molecular emission dipole (here, absorption and emission dipoles are collinear). The azimuthal angle, ϕ, is the angle made with respect to x in the x-y plane. b) Intensity and *A(t)* trajectories for R6G on brush at pH 7, showing repeated polarization state switching of an absorbed molecule. c) and d) additional single molecule trajectories for R6G, with representative traces of diffusion behaviors.

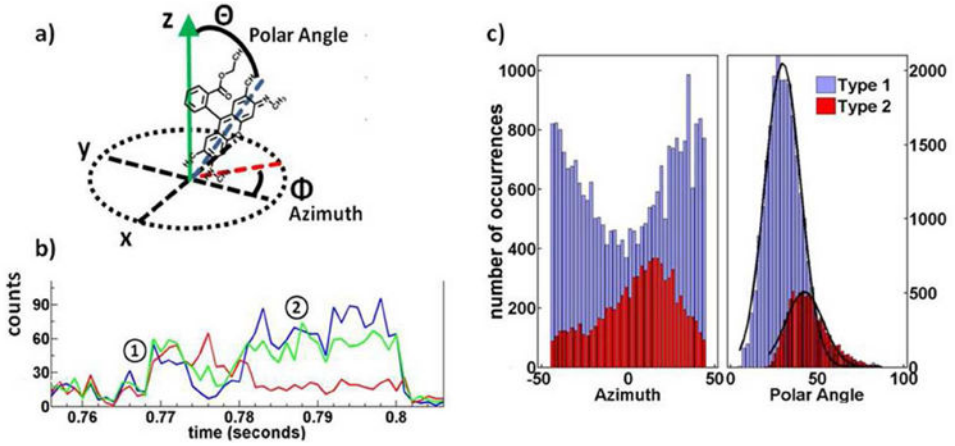

Figure 4.

a) Coordinate scheme, with R6G and emission dipole depicted. b) A close-up of a single molecule transition through the laser focal volume, showing the intensity traces acquired from the three detectors. Region labeled Type 1: Nonoriented diffusion with rapid reorientation. Region labeled Type 2: Oriented diffusion with restricted rotation. c) Distribution of R6G azimuthal and polar angles, respectively, sampled in the polymer brush, measured over all diffusion events during a 5 minute period. The two types of diffusion, non-oriented, signified as Type 1, and oriented, Type 2, are shown in the separate purple and red histograms respectively. The polar angle distributions are well fit by a Gaussian. The azimuthal angle distributions hint at a number of subpopulations and fits with up to 4 Gaussians do not converge. Capital Θ and Φ, as shown, are the *actual* polar and azimuthal angles, respectively, adopted by a dipole.

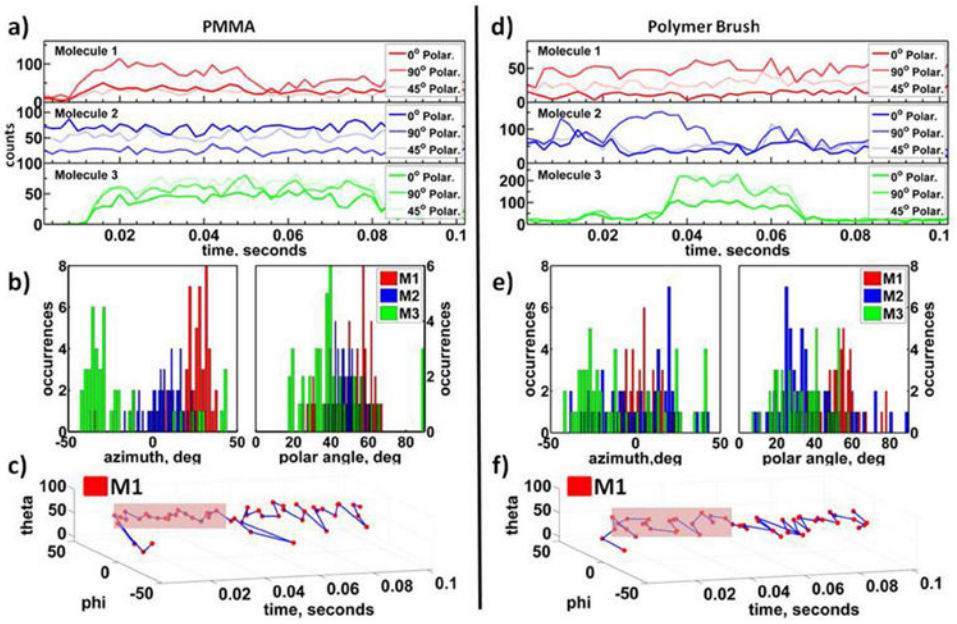

Figure 5.

(left) Data for 3 different single molecule events for R6G embedded in PMMA is shown, a) intensity traces, b) distributions of sampled angles for the three events, c) a scatter plot for the top trace in a) over the time course shown. (right) Data for R6G events in polymer brush, with intensity traces, angle distributions and scatter plots in d-f. The highlighted region in part c shows a portion of the trajectory from which the maximum standard deviation due to instrument noise can be estimated. The highlighted region in part f) shows a region of repeating oscillation.

Table 1

Diffusion times for R6G, Bodipy-R6G, and Alexa 555, through a confocal laser volume, in the presence of polymer brush.

Dye (charge)	Slow Diffusion (ms)	Intermediate Diffusion (ms)	Bulk Like Diffusion (ms)
R6G (+)	240 ± 30	4 ± 2.5	×
Bodipy (0)	60 ± 24	4 ± 2.3	×
Alexa (-)	×	2.5 ± 0.6	0.032 ± 0.001